

Online Learning and Control Synthesis for Reachable Paths of Unknown Nonlinear Systems

Yiming Meng, Taha Shafa, Jesse Wei, Melkior Ornik *Senior Member, IEEE*

Abstract—In this paper, we present a novel method to drive a nonlinear system to a desired state, with limited a priori knowledge of its dynamic model: local dynamics at a single point and the bounds on the rate of change of these dynamics. This method synthesizes control actions by utilizing locally learned dynamics along a trajectory, based on data available up to that moment, and known proxy dynamics, which can generate an underapproximation of the unknown system’s true reachable set. An important benefit to the contributions of this paper is the lack of knowledge needed to execute the presented control method. We establish sufficient conditions to ensure that a controlled trajectory reaches a small neighborhood of any provably reachable state within a short time horizon, with precision dependent on the tunable parameters of these conditions.

Index Terms—Control Synthesis; Model-Free Nonlinear Systems; Online Learning; Guaranteed Reachability.

I. INTRODUCTION

Systems across domains operate with limited information, such as uncertainties arising from an insufficient understanding of system transitions and external forces.

In this paper, we focus on the situation where the nonlinear system is partially unknown, with our knowledge limited to its local dynamics at a single point and the bounds on the rate of change of these dynamics. Based on this restricted information, we aim to implement the following pipeline for the system. First, we identify a set of states, known as the Guaranteed Reachable Set (GRS), that the unknown system can provably reach within a given timeframe from the point of known information, using underapproximation proxy dynamics [1], [2]. Then, we specify a state on the boundary of the GRS and synthesize a controller, enabling the partially unknown system to approach the vicinity of this state. Although the works in [1], [2] provide a systematic method for estimating the GRS based on set-valued mapping analysis, they lack the capability to conversely identify a control signal that maneuvers the true system to reach a specified region within the GRS. Therefore, we concentrate on addressing the question of how to design control for the reachability task mentioned above.

This research was supported by NASA under grant numbers 80NSSC21K1030 and 80NSSC22M0070, as well as by the Air Force Office of Scientific Research under grant number FA9550-23-1-0131.

Yiming Meng is with the Coordinated Science Laboratory, University of Illinois Urbana-Champaign, Urbana, IL 61801, USA. [ymmeng@illinois.edu](mailto:yymmeng@illinois.edu).

Taha Shafa and Jesse Wei are with the Department of Aerospace Engineering, University of Illinois Urbana-Champaign, Urbana, IL 61801, USA. tahaas2@illinois.edu, jwei28@illinois.edu.

Melkior Ornik is with the Department of Aerospace Engineering and the Coordinated Science Laboratory, University of Illinois Urbana-Champaign, Urbana, IL 61801, USA. mornik@illinois.edu.

Motivated by scenarios where an adverse event can cause significant changes to the system dynamics, there exists a substantial body of work in the realm of control for systems with uncertainties in the dynamic model. Data-driven and neural network control methods [3]–[6] can be utilized for applications that include computing steady-state transfer functions in real-time or synthesizing controllers for nonlinear systems with dynamic modeling uncertainties. Other methods involve learning a Gaussian process model [7], [8] for black-box identification of nonlinear systems. Methods outside of identification [9]–[15] and machine learning methods [16], [17] utilize control tools like control barrier functions [18] and more classical adaptive control methods [19]–[21], but are limited to handling less significant uncertainties. While all of these methods have their merits, they all require the use of significantly more information, such as an existing model with uncertainties or system data.

In contrast, the novel control method we present for online controller synthesis relies solely on discrete-time, up-to-date historical data from a single trajectory run and a derived underapproximation proxy control system based on presumed model information [1], [2]. It is worth noting that the work [22] is capable of learning dynamics and potentially achieving the specified control tasks, such as reachability and safety, using the same data. However, a ‘goodness function’—encoding side information about the system, such as physical laws—must be carefully designed to ensure that the controlled trajectory moves in a nearly optimal direction. The key difference highlighted in this paper is that we can utilize the knowledge of the GRS and the proxy system that generates it for control design. This framework relaxes the requirement for potential side information from the unknown system and provides a reachability guarantee.

The outline of this paper is as follows. In Section II, we discuss the preliminary knowledge we assume, which is in line with assumptions in [1], [2]. In Section III, we show the necessary properties of the underapproximated proxy control system, particularly in identifying a path to a provably reachable desired state, which serves as a reference trajectory for the original system to follow. In Section IV, we prove that the proposed framework enables the true system’s state to track the reference path and converge to the desired state. We then present an algorithm for applying this control method. Lastly, we conduct a case study to investigate the effectiveness of the proposed algorithm, as detailed in Section V.

Notation: We denote the Euclidean space by \mathbb{R}^d for $d > 1$. We denote \mathbb{R} the set of real numbers, and $\mathbb{R}_{\geq 0}$ the set of nonnegative real numbers. The closed ball of radius r centered

at $x \in \mathbb{R}^d$ is denoted by $\mathcal{B}^d(x; r) := \{y \in \mathbb{R}^d : |y - x| \leq r\}$, where $|\cdot|$ is the Euclidean norm. For a given set $A \subseteq \mathbb{R}^d$, $\text{Int}(A)$ denotes its interior, and ∂A denotes its boundary. For a closed set $A \subseteq \mathbb{R}^d$ and $x \in \mathbb{R}^d$, we denote the distance from x to A by $|x|_A = \inf_{y \in A} |x - y|$. For a matrix M , $\|M\|$ denotes its Euclidean norm: $\|M\| = \sup_{|v|=1} |Mv|$, M^\dagger denotes the Moore-Penrose pseudoinverse, $\text{Im}(M)$ denotes the image. For matrices M and N , we say $M \in \text{Imm}(N)$ if all columns of M lie in $\text{Im}(N)$.

II. PRELIMINARIES

Let the admissible set of inputs be $\mathcal{U} = \mathcal{B}^m(0; 1)$, which is a common setting in reachability analysis [23], [24]. We consider the following unknown dynamical system defined by

$$\dot{\mathbf{x}}(t) = f(\mathbf{x}(t)) + G(\mathbf{x}(t))\mathbf{u}(t), \quad \mathbf{x}(0) = x_0, \quad (1)$$

where for all $t \geq 0$, $\mathbf{x}(t) \in \mathbb{R}^d$; $\mathbf{u} : \mathbb{R}_{\geq 0} \rightarrow \mathcal{U}$. The mappings $f : \mathbb{R}^d \rightarrow \mathbb{R}^d$, and $G : \mathbb{R}^d \rightarrow \mathbb{R}^{d \times m}$ are Lipschitz continuous with Lipschitz constants $L_f, L_G \geq 0$. We introduce $L_0 := \max\{L_f, L_G\}$ for future references.

For any initial condition $x_0 \in \mathbb{R}^d$, we denote by $\phi_{\mathbf{u}}(\cdot, x_0) : [0, \infty) \rightarrow \mathbb{R}^d$ the controlled flow map (solution) under \mathbf{u} , and by $\Phi(x_0; \mathcal{U})$ the set of solutions. We simply use $\phi_{\mathbf{u}}(\cdot)$ if we do not emphasize the initial condition. For any $T \geq 0$, the set of states reached by solutions starting from x_0 at time T is defined as $\mathcal{R}^T(x_0) := \{\phi_{\mathbf{u}}(T) : \phi_{\mathbf{u}}(\cdot) \in \Phi(x_0; \mathcal{U})\}$, and we also define the reachable set as $\mathcal{R}^{\leq T}(x_0) := \cup_{t \in [0, T]} \mathcal{R}^t(x_0)$.

For the reachability analysis and control synthesis, we propose the following hypotheses that are consistent with those presented in [2, Section II.A]: (H1) f and G are of the form $f(x) = Bh(x)$ and $G(x) = BH(x)$ where $B \in \mathbb{R}^{d \times m}$ is a constant matrix, $h : \mathbb{R}^d \rightarrow \mathbb{R}^m$, and $H : \mathbb{R}^d \rightarrow \mathbb{R}^{m \times m}$ such that $H(x_0)$ is invertible; (H2) L_f and L_G are known, as well as values $f(x_0)$ and $G(x_0)$ such that $G(x_0) \neq 0$. We also assume knowledge of $\text{Im}(B)$ and $\text{Imm}(B)$. However, we do not need to know the value of B exactly.

For convenience, we denote by \mathcal{D}_{con} the set of all pairs f and G consistent with H1 and H2 for the same L_f and L_G . We also denote $C := \|G(x_0)\| \|G(x_0)^\dagger\|$.

Remark 2.1: The settings are motivated by situations where damage to a system can alter its dynamics, with these changes captured by system (1). In practice, an online approximation of $f(x_0)$ and $G(x_0)$ can be achieved with sufficient accuracy [22], [25]. However, for clearer illustration, we assume that the information at x_0 is perfectly known, allowing us to further explore the system's remaining capabilities.

Additionally, the recent work in [26] extends [1], [2] to Riemann manifolds, with applications for underactuated systems. This paper presents a control synthesis technique based on (H1) and (H2), with plans to generalize it based on more relaxed conditions for f and G given insights from [26]. \diamond

III. Underapproximated Proxy Control System and Its Reachable Paths

With limited knowledge about the system dynamics, we attempt to construct a control signal to reach a small neighborhood of a specified point on the boundary of the GRS, which is contained within the true reachable set. In this section, we

revisit the underapproximated proxy control system for GRS evaluation [2], which can be viewed as supplementary information for the above reachability control problem. Particularly, we highlight the connections to the actual system (1). Then, we investigate properties related to the reachable paths and their corresponding control signals for the proxy system.

A. The Proxy System

The underapproximated proxy control system is obtained through a connection to (1) as shown in [2, Theorem 1]. We rephrase the statement as follows.

Theorem 3.1: Let \mathcal{U} , L_f , and L_G be given. Then, there exists a $u \in \mathcal{U}$ satisfying

$$k\hat{u} = f(x) - f(x_0) + G(x)u \quad (2)$$

for all $x \in \mathbb{B} := \{x : |x| \leq \|G(x_0)^\dagger\|^{-1} / (L_f + L_G)\}$, any $\hat{u} \in \mathcal{B}^d(0; 1) \cap \text{Im}(G(x_0))$, and any k such that $|k| \leq \|G(x_0)^\dagger\|^{-1} - (L_f + L_G)|x|$. \diamond

Consequently, by [2, Theorem 3], the GRS of (1) can be calculated based on a proxy equation of the form

$$\dot{\hat{\mathbf{x}}}(t) = a + (b - c|\hat{\mathbf{x}}(t)|)\hat{\mathbf{u}}(t), \quad \hat{\mathbf{x}}(0) = x_0, \quad (3)$$

on the domain \mathbb{B} , where $a = f(x_0)$, $b := \|G(x_0)^\dagger\|^{-1}$, $c := L_f + L_G$, and $\hat{\mathbf{u}} : [0, \infty) \rightarrow \hat{\mathcal{U}}$ for $\hat{\mathcal{U}} = \mathcal{B}^d(0; 1) \cap \text{Im}(G(x_0))$. It can also be verified from (H1) and (H2) that $a \in \text{Im}(G(x_0))$ [2]. For any $x_0 \in \text{Int}(\mathbb{B})$, we denote by $\hat{\phi}_{\hat{\mathbf{u}}}(\cdot, x_0) : [0, \infty) \rightarrow \mathbb{R}^d$ the controlled flow map (solution) under $\hat{\mathbf{u}}$, by $\hat{\Phi}(x_0; \hat{\mathcal{U}})$ the set of solutions. We also use $\hat{\phi}_{\hat{\mathbf{u}}}(\cdot)$ to denote the solution when the initial condition is not emphasized. Let $T \geq 0$, the reachable set at time T and up to T (i.e., the GRS up to T) are denoted by $\hat{\mathcal{R}}^T(x_0)$ and $\hat{\mathcal{R}}^{\leq T}(x_0)$, respectively.

Then, for all $T \geq 0$ and all $x_0 \in \mathbb{B}$, $\hat{\mathcal{R}}^{\leq T}(x_0) \subseteq \mathcal{R}^{\leq T}(x_0)$. Eq. (3) demonstrates the ‘slowest’ growing rate for all $(f, G) \in \mathcal{D}_{\text{con}}$. It is worth noting that the proxy system (3) is not an approximation of the true dynamics. For simplicity, we assume $x_0 = 0$. Otherwise, shifting coordinates via $\tilde{x} = x - x_0$ yields $\dot{\tilde{x}} = \tilde{f}(\tilde{x}) + \tilde{G}(\tilde{x})u$, with $\tilde{f}(\tilde{x}) = f(\tilde{x} + x_0)$, $\tilde{G}(\tilde{x}) = G(\tilde{x} + x_0)$, and $\tilde{x}_0 = 0$. The parameters $a = \tilde{f}(0)$, $b = \|\tilde{G}(0)^\dagger\|^{-1}$, and c in the proxy dynamics after the coordinate shift remain unchanged.

B. Reachable Path of the Proxy System

In view of Theorem 3.1, for any path generated by (3), there always exists a control signal \mathbf{u} for (1) that ensures the system to follow the same path. This motivates us to identify a valid reachable path generated by system (3), which can approach a small neighborhood of a target point on the boundary of GRS. To do this, we investigate the proxy system in this subsection beyond the properties stated in [2], specifically for the purpose of control synthesis. Below, we present some facts for (3). The proofs can be found in Appendix A.

Proposition 3.2: We assume that there exists a $\Omega \subseteq \mathbb{B}$ such that $|a| < b - c \cdot \sup_{x \in \Omega} |x|$. Consider system (3) on Ω . Let T be such that $\hat{\mathcal{R}}^{\leq T}(x_0) \subseteq \Omega$. Then, for any $y \in \partial \hat{\mathcal{R}}^{\leq T}(x_0)$, $\exists \hat{\phi}_{\hat{\mathbf{u}}}(\cdot) \in \hat{\Phi}(x_0; \hat{\mathcal{U}})$ such that $\hat{\phi}_{\hat{\mathbf{u}}}(t) = y$ for any $t \in [0, T)$. \diamond

The above property states that $\hat{\mathcal{R}}^{\leq T}(x_0)$ expands monotonically as T increases for relatively small $|a|$ ¹. We therefore intend to work with $\partial\hat{\mathcal{R}}^T(x_0)$ rather than $\partial\hat{\mathcal{R}}^{\leq T}(x_0)$. In terms of computing $\partial\hat{\mathcal{R}}^T(x_0)$, although existing methods offer guaranteed precision [27]–[29], they require long computation times and are unsuitable for online learning and control synthesis. We thus introduce $\partial\hat{\mathcal{R}}_{\text{pse}}^T(x_0) := \{\hat{\phi}_{\hat{\mathbf{u}}}(T) : \hat{\mathbf{u}} \equiv \nu, \nu \in \partial\hat{\mathcal{U}}\}$ and adopt a Monte Carlo method for its computation.

Proposition 3.3: Given a T such that $\hat{\mathcal{R}}^{\leq T}(x_0) \subseteq \text{Int}(\mathbb{B})$. Then, for $a = 0$, $\partial\hat{\mathcal{R}}_{\text{pse}}^T(x_0) = \partial\hat{\mathcal{R}}^T(x_0)$. Consequently, for any $y \in \partial\hat{\mathcal{R}}^T(x_0)$, it can be reached under $\hat{\mathbf{u}} \equiv \frac{y}{|y|}$. \diamond

When $a \neq 0$, $\partial\hat{\mathcal{R}}_{\text{pse}}^T(x_0)$ is generally not equal to $\partial\hat{\mathcal{R}}^T(x_0)$ ². However, we have the following approximation.

Proposition 3.4: Consider $\hat{\mathbf{x}}(t) = (b - c|\hat{\mathbf{x}}(t)|)\hat{\mathbf{u}}(t)$ and its solution $\bar{\phi}_{\hat{\mathbf{u}}}(t)$. Then, it follows that $\vartheta_a(t) := |\hat{\phi}_{\hat{\mathbf{u}}}(t) - \bar{\phi}_{\hat{\mathbf{u}}}(t) - at| \leq \frac{e^{ct} - (1+ct)}{c}|a|$. \diamond

Now, we denote $\hat{\mathcal{R}}^T(x_0)$ as the reachable set for the driftless $\bar{\phi}(\cdot)$ at T . As a direct consequence of Proposition 3.2–3.4, for any $y \in \partial\hat{\mathcal{R}}^T(x_0)$, there exists a control $\hat{\mathbf{u}}$ such that $\hat{\phi}_{\hat{\mathbf{u}}}(T) = y$, and hence $y \in \{x \in \mathbb{R}^n : |x|_{\partial\hat{\mathcal{R}}^T(x_0)+aT} \leq \vartheta_a(T)\}$. By the same logic, for any $y \in \partial\hat{\mathcal{R}}^T(x_0) + aT$, we have $y \in \{x \in \mathbb{R}^n : |x|_{\partial\hat{\mathcal{R}}^T(x_0)} \leq \vartheta_a(T)\}$. Therefore, in the Hausdorff distance, $d_H(\partial\hat{\mathcal{R}}^T(x_0) + aT - \partial\hat{\mathcal{R}}^T(x_0)) \leq \vartheta_a(T)$. Similarly, one can apply Proposition 3.3 and show that $d_H(\partial\hat{\mathcal{R}}^T(x_0) + aT - \partial\hat{\mathcal{R}}_{\text{pse}}^T(x_0)) \leq \vartheta_a(T)$. Note that, for sufficiently small T , $\vartheta_a(T)$ is approximately bounded by $|a| \cdot (T^2/2 + \mathcal{O}(T^3))$.

Let $\rho := \sup_{x \in \hat{\mathcal{R}}_{\text{pse}}^T(x_0)} |x|$ and $\Delta_a := \frac{|a|}{b - c\rho}$. For the remainder of the paper, we focus on the scenario where $\partial\hat{\mathcal{R}}_{\text{pse}}^T(x_0) \subseteq \mathbb{B}$ and $\Delta_a < 1$. Note that for any $y \in \partial\hat{\mathcal{R}}_{\text{pse}}^T(x_0) \subseteq \text{int}(\mathbb{B})$, as verified by the definition of $\partial\hat{\mathcal{R}}_{\text{pse}}^T(x_0)$, one can use $\hat{\mathbf{u}} \equiv \frac{y - aT}{|y - aT|}$ in the proxy system to reach y . On the other hand, based on the above facts about approximations using the driftless proxy system (which enable easier computation), we can verify that the trajectory created by $\hat{\mathbf{u}} \equiv \frac{y - aT}{|y - aT|}$ deviates from the straight-line segment toward y by no more than $\frac{cT^2}{2} \sqrt{|a|^2 - \langle a, y \rangle^2 / |y|^2} + \mathcal{O}(T^3)$, provided that T is sufficiently small relative to $|a|$. One can then directly use the straight-line segment toward y as the reference path for control synthesis in the next section, enabling simpler analysis and computation.

IV. CONTROL SYNTHESIS

In this section, our objective is to synthesize a controller that leads the trajectory to eventually reach a neighborhood of a specified $\partial\hat{\mathcal{R}}_{\text{pse}}^T(x_0)$ for some $T > 0$. We take advantage of the properties of (3) as stated in Section III and search for control inputs for the system (1) such that $\phi_{\mathbf{u}}(t)$ follows the reference path toward y with the same velocity as $\hat{\phi}_{\hat{\mathbf{u}}}(t)$.

¹For values of a that do not satisfy the condition in Proposition 3.2, specifying a point on $\partial\hat{\mathcal{R}}^{\leq T}(x_0)$ may result in the point being reached at some $t < T$ due to the strong drift. Additionally, the predicted GRS significantly deviates from the true reachable set, even over a short time horizon, as demonstrated in [2, Section V.A]. Therefore, it would be less practical to consider the same reachability control task as discussed in the remainder of this article based on the knowledge of the GRS. Nevertheless, we provide a reachability analysis in Appendix D.

²We kindly refer readers to Appendix C and Proposition C.1 for counterexample, which indicate that the control signal that maneuvers $\hat{\phi}_{\hat{\mathbf{u}}}$ to the boundary of the GRS always has full magnitude, but its direction may vary over time.

In practice, however, it is impossible to accurately learn the transition of (1) based on a single system run, and hence achieving an exact path-following strategy is unattainable. Considering this situation, to leverage the connection between systems (1) and (3) and fully utilize the known information, we must necessarily relax the reachable time $T > 0$; that is, we consider finite-time reachability rather than reachability at the exact time T . We create a ‘correct-by-construction’ reference path from (3), based on up-to-date trajectory information.

Furthermore, due to the limited information and potential nonlinearity of f and G , long-term predictability of the trajectory is not achievable. The controllers must provide infinitesimal direction to constantly track the reference path, which will in turn force the controlled $\phi_{\mathbf{u}}(t)$ to be maintained within a small neighborhood of the reference path. To better illustrate the idea, we focus on the case where $a = 0$.

A. Preliminaries for System Learning

In order to learn $f(x) + G(x)u$ at points along any single-run trajectory, we consider a piece-wise constant control \mathbf{u} , where each piece has a duration of δt . To be more specific, the controller can apply any $m + 1$ affinely independent constant inputs for a short period of time δt [22]. Thus, the entire learn-control cycle is of length $\tau = (m + 1)\delta t$.

Let $\tau_n := n\tau$ for $n \in \mathbb{N}$, and let $\{\tau_n\}_n$ be the sequence of instants at which to decide velocity. Consider the index sets $\mathcal{I} := \{0, 1, \dots, m\}$ and $\mathcal{I}_0 := \{1, 2, \dots, m\}$. We then denote $\{u_{n,j}\}_{j \in \mathcal{I}}$ by the affinely independent sequence of constant inputs, where $u_{n,j}$ is applied within $[\tau_n + j\delta t, \tau_n + (j + 1)\delta t)$ for each $j \in \mathcal{I}$. In this case, each $u_{n,0}$ is determined at τ_n by a strategy aimed at returning a nearly optimal direction attracted to the reference path. Meanwhile, $\{u_{n,j}\}_{j \in \mathcal{I}_0}$ are subsequent inputs that are selected according to a fixed procedure.

We propose the following inductive procedures to achieve the control task, with a detailed explanation of their feasibility. The proofs can be found in Appendix B.

B. Learning of System Dynamics

Suppose that $u_{n,0}$ has been determined at τ_n for each n . We then proceed to learn the system dynamics, denoted as $v_x(u) := f(x) + G(x)u$ at τ_{n+1} for each n . We follow the learning algorithm in the reference [22, Section V], which is based on the trajectory information within each learn-control cycle, spanning the interval $[\tau_n, \tau_{n+1})$. This is achieved by leveraging the control affine form of system (1), and by employing an affinely independent sequence of constant inputs

$$u_{n,j} := u_{n,0} + \Delta u_j \quad (4)$$

within $[\tau_n + j\delta t, \tau_n + (j + 1)\delta t)$ for each $j \in \mathcal{I}_0$. Here, $\Delta u_j := \pm \epsilon \mathbf{e}_j$, for $\epsilon > 0$ representing a small amplitude, and $\{\mathbf{e}_j\}_{j \in \mathcal{I}_0}$ being the set of orthonormal unit vectors in \mathbb{R}^m .

Denote $M_0 := \max\{\sup_{x \in \mathbb{B}} |f(x)|, \sup_{x \in \mathbb{B}} |G(x)|\}$, $C_0 := M_0(m + 1)$, $C_1 := M_0(m + 1)^2$, $C_2 := 2M_0L_0(m + 1)^2$, and $C_3 := M_0L_0(m + 1)^3$. Let $x_{n,j} = \phi_{\mathbf{u}}(\tau_n + j\delta t, x_0)$ and $\mathbf{x}_{n+1} := x_{n,m+1}$. Then, it is clear that $\mathbf{x}_{n+1} = x_{n+1,0}$. We have the following approximation precision [22, Lemma 4]:

- (1) $|\phi_{\mathbf{u}}(t_1, x_0) - \phi_{\mathbf{u}}(t_2, x_0)| \leq C_0|t_2 - t_1|, \forall t_1, t_2 \in [\tau_n, \tau_{n+1}]$. In particular, $|\mathbf{x}_{n+1} - \mathbf{x}_n| \leq C_1 \cdot \delta t$;
- (2) $|\frac{(x_{n,j+1} - x_{n,j})}{\delta t} - v_{x_{n,j+1}}(u_{n,j})| \leq (C_2/4) \cdot \delta t, \forall j \in \mathcal{I}$.
- (3) $|v_{x_{n,j+1}}(u_{n,j}) - v_{\mathbf{x}_{n+1}}(u_{n,j})| \leq C_3 \cdot \delta t, \forall j \in \mathcal{I}$.

By introducing the following class of parameterized control inputs, we can approximate the system dynamics using only the information from the trajectory data and the parameters.

Definition 4.1: Let $\Lambda := \{\lambda = \{\lambda_j\}_{j \in \mathcal{I}} \subseteq \mathbb{R}_{\geq 0} : \sum_{j \in \mathcal{I}} \lambda_j = 1\}$. A parameterized control input w.r.t. $\lambda \in \Lambda$ is of the form $u_{n,\lambda} := \sum_{j \in \mathcal{I}} \lambda_j u_{n,j}$. We define the set of parameterized control inputs as $\mathcal{U}_{n,\lambda} := \{u_{n,\lambda} \in \mathcal{U} : \lambda \in \Lambda\}$. \diamond

Note that, by [22, Theorem 5], we have the following bound $|v_{\mathbf{x}_{n+1}}(u_{\lambda}) - \sum_{j \in \mathcal{I}} \lambda_j (x_{n,j+1} - x_{n,j})/\delta t| \leq \mathcal{E}_{\lambda}(\delta t, \epsilon)$ for $u_{n,\lambda} \in \mathcal{U}_{n,\lambda}$ and $\mathcal{E}_{\lambda}(\delta t, \epsilon) = 2((4m^{\frac{3}{2}} + \epsilon)/\epsilon) \cdot C_3 \cdot \delta t$. This bound, which depends on two parameters, indicates the necessity of considering their joint effect to converge to 0, rather than adjusting each parameter individually. We then use the approximation $\hat{v}_{\mathbf{x}_{n+1}}(u_{n,\lambda}) := \sum_{j \in \mathcal{I}} \lambda_j (x_{n,j+1} - x_{n,j})/\delta t$ of $v_{\mathbf{x}_{n+1}}(u_{n,\lambda})$ for the decision-making at τ_{n+1} .

C. Control Design at τ_n

1) *Initial Control Input:* For $n = 0$, the control input $u_{0,0}$ is considered to initialize the system (1), such that the direction of unknown system within $[0, \delta t]$ is expected to closely follow that of the proxy system (3). As $f(x_0)$ and $G(x_0)$ are known, we use the following argument to determine $u_{0,0}$. Since $\delta t > 0$ is arbitrarily small, we have $\phi_{\mathbf{u}}(\delta t) = \delta t \cdot (f(x_0) + G(x_0)u_{0,0}) + \mathcal{O}(\delta t^2) = \delta t \cdot (G(x_0)u_{0,0}) + \mathcal{O}(\delta t^2)$, where $\mathcal{O}(\delta t^2)$ is a high order term w.r.t. δt . On the other hand, in view of Proposition 3.3, the control $\hat{\mathbf{u}}$ leading to the optimal direction for the proxy system (3) is the constant signal $\hat{\mathbf{u}} \equiv \frac{y}{|y|}$. Therefore, $\hat{\phi}_{\hat{\mathbf{u}}}(\delta t) = \frac{y}{|y|} \cdot \int_0^{\delta t} (b - c|\hat{\phi}_{\hat{\mathbf{u}}}(s)|) ds = (1 - \epsilon) \frac{b \cdot y \cdot \delta t}{|y|} + \epsilon \frac{b \cdot y \cdot \delta t}{|y|} + \mathcal{O}(\delta t^2)$, recalling $b := \|G(x_0)^{\dagger}\|^{-1}$ and $c := L_f + L_G$. The parameter $\epsilon > 0$, representing a small amplitude used in Equation (4), is reserved for future attempts to employ multiple small-wiggling, independent inputs $\{\Delta u_j\}$ for learning the dynamics, as discussed in Section IV-B. By equating the first-order terms, $\delta t \cdot (G(x_0)u_{0,0}) = (1 - \epsilon)b \cdot y \cdot \delta t/|y|$, we can set the initial constant control $u_{0,0} = (1 - \epsilon) \frac{G(x_0)^{\dagger}(y)}{\|G(x_0)^{\dagger}\| |y|}$ for the system (1). Recalling (4), the term $1 - \epsilon$ is used to ensure that the sequence $\{u_{0,j}\}$ is a subset of \mathcal{U} .

2) *Control Design at Other τ_n :* Recall notations in IV-B. We aim to create a sequence $\{z_n\}$, such that $z_n = \theta_n y$ and $\{\theta_n\}$ is an increasing sequence of real numbers within $[0, 1]$ converging to 1. Then, within each learning cycle, we design control inputs to ensure that $\phi_{\mathbf{u}}(t)$ approaches each z_n . In order to dynamically measure the distance of $\phi_{\mathbf{u}}(t)$ with the reference path, we now introduce the function $d_z(x) = |x - z|^2$ for $z = \theta y$ and $\theta \in [0, 1]$.

To guarantee feasibility, we need to demonstrate that the sequence $\{z_n\}$, which satisfies the previously mentioned property, can be constructed based on the trajectory data. Furthermore, for any $t \in (\tau_n, \tau_{n+1})$, there should exist $\{u_{n,0}\}$ (along with $\{u_{n,j}\}$ introduced in Section IV-B) that also satisfies

$$\dot{d}_{z_n}(\phi_{\mathbf{u}}(t)) = \langle \nabla d_{z_n}(\phi_{\mathbf{u}}(t)), v_{\phi_{\mathbf{u}}(t)}(\mathbf{u}(t)) \rangle < 0. \quad (5)$$

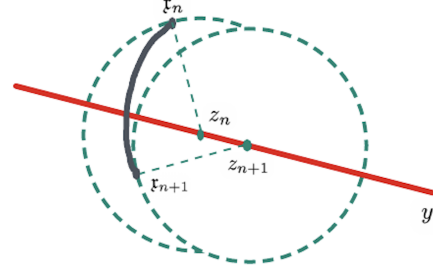


Fig. 1. An illustration of Lemma 4.2. The point z_n is given as the point on the line segment between 0 and y with $|z_n - \mathbf{x}_n| = r$. Suppose $\dot{d}_{z_n}(\phi_{\mathbf{u}}(t)) < 0$ for all $t \in [\tau_n, \tau_{n+1})$, then $|\mathbf{x}_{n+1} - z_n| < r$, and z_{n+1} can be found on the line segment with $|z_{n+1} - \mathbf{x}_{n+1}| = r$ and moves closer to y .

We first argue inductively to show that the above properties can be satisfied. We also refer to Figure 1 for a visualization.

Lemma 4.2: Let $n \geq 1$ and $r > 0$ be fixed. Let $\mathbf{u}(t) = u_{n,j}$ for $t \in [\tau_n + j\delta t, \tau_n + (j+1)\delta t)$ and for $j \in \mathcal{I}$. Let \mathbf{x}_n be given and consider $z_n = \theta_n y$ with $|z_n - \mathbf{x}_n| = r$ for some $\theta_n \in (0, 1)$. Suppose that $\dot{d}_{z_n}(\phi_{\mathbf{u}}(t)) < 0$ for all $t \in [\tau_n, \tau_{n+1})$. Then, there exists a $z_{n+1} = \theta_{n+1} y$ such that $\theta_{n+1} > \theta_n$ and $|z_{n+1} - \mathbf{x}_{n+1}| = r$. Particularly, $r - |\mathbf{x}_{n+1} - z_n| \leq |z_{n+1} - z_n| < 2r$. \diamond

It then suffices to show that there exists a determination strategy for r , ϵ , and δt , such that the above construction of $\{z_n\}$ can be initialized, and there exists $\{u_{n,0}\}$ such that $\dot{d}_{z_n}(\phi_{\mathbf{u}}(t)) < 0$ for all $t \in [\tau_n, \tau_{n+1})$. In selecting r to incorporate the learning process described in Section IV-B, we consider the quantity $r := r(k, \delta t) = \sup_{\{\hat{\mathbf{u}} \equiv \hat{u} \in \partial \mathcal{U}\}} |\hat{\phi}_{\hat{\mathbf{u}}}(k\tau, x_0) - x_0|$. The following lemma provides a set of conditions on k , ϵ , and δt under which the sequence z_n can be initialized; these conditions can always be satisfied through appropriate tuning, particularly with sufficiently small ϵ and δt .

Lemma 4.3: Let $\mathbf{u}(t) = u_{0,j}$ for $t \in [j\delta t, (j+1)\delta t)$ and for $j \in \mathcal{I}$. Consider $z_0 = x_0 = 0$. Suppose ϵ and δt satisfy $\epsilon > (C_3/C)\delta t$. Recall $\rho := \sup_{\{x \in \mathcal{R}_{\text{pre}}^T(x_0)\}} |x|$. If we also have $k > Cb/(b - c\rho)$ and $2kb\tau/(b - c\rho) < T$, then, there exists a $z_1 = \theta_1 y$ such that $\theta_1 \in (0, 1)$ and $|z_1 - \mathbf{x}_1| = r := r(k, \delta t)$. \diamond

We now show the existence of $u_{n,0}$ such that (5) holds for all n . The following statement verifies the existence of the control input for (1) such that (5) is satisfied at τ_n .

Proposition 4.4: For each $n \geq 1$, let \mathbf{x}_n be given and z_n be determined by Lemma 4.2 with $r := r(k, \delta t)$. Then, there exist a $u \in \mathcal{U}$ such that $\langle \nabla d_{z_n}(\mathbf{x}_n), f(\mathbf{x}_n) + G(\mathbf{x}_n)u \rangle \leq -2r(b - c|\mathbf{x}_n|)$. Particularly, we can determine u as $\text{argmin}_{u \in \mathcal{U}} \langle \nabla d_{z_n}(\mathbf{x}_n), f(\mathbf{x}_n) + G(\mathbf{x}_n)u \rangle$. \diamond

We then continue to show that, within each learning cycle $[\tau_n, \tau_{n+1})$, by considering the subsequential small-wiggling inputs $\{\Delta u_j\}$ as described in Section IV-B, we have $\dot{d}_{z_n}(\phi_{\mathbf{u}}(t)) < 0$ for all $t \in [\tau_n, \tau_{n+1})$ for small δt and ϵ .

Theorem 4.5: Recall notation b and c in (3). Define $\mathcal{E}_r(\delta t, \epsilon) := C_2\delta t + \epsilon M_0$ and $\mathcal{E}_n(\delta t, \epsilon) := 2M_0C_1\delta t + C_1\mathcal{E}_r(\delta t, \epsilon)$. Suppose that $\mathcal{E}_n(\delta t, \epsilon) \leq r(b - c|\mathbf{x}_n| - \mathcal{E}_r(\delta t, \epsilon))$. Let $\mathbf{u}(\tau_n) = u$ be the control input as in Proposition 4.4. Let $\mathbf{u}(t) = u_{n,j}$ for all $t \in [\tau_n + j\delta t, \tau_n + (j+1)\delta t)$ and for each $j \in \mathcal{I}$. Then $\dot{d}_{z_n}(\phi_{\mathbf{u}}(t)) < 0$ for all $t \in [\tau_n, \tau_{n+1})$. \diamond

Remark 4.6: For $t \in [\tau_n, \tau_{n+1})$, the deviation $|\phi_{\mathbf{u}}(t) - \mathbf{x}_n|$ should be small as presented in [22, Lemma 4]. Consequently, the uncertain deviations $|f(\phi_{\mathbf{u}}(t)) - f(\mathbf{x}_n)|$ and $|G(\phi_{\mathbf{u}}(t)) - G(\mathbf{x}_n)|$ are small. The condition on the small terms \mathcal{E}_n and \mathcal{E}_r ensures that the attracting force $-2r(b - c|\mathbf{x}_n|)$ at each τ_n (as in Proposition 4.4) continues to dominate over the interval (τ_n, τ_{n+1}) , so that the flow remains attracted to z_n even in the presence of such uncertainty.

Recalling that $r = r(k, \delta t)$ represents the maximal length of $\phi_{\mathbf{u}}(k\tau, x_0)$ under constant inputs for (3), to satisfy the stated condition, one needs consider the joint effect of k and δt . Note that for δt sufficiently small, $r \approx kb\tau$. For small b and $k = 1$, the main contributor $2M_0C_1\delta t \leq r(b - c|\mathbf{x}_n|)$ in the condition stated in Theorem 4.5 may not hold. However, this is not problem in view of the proof of Lemma 4.3. We consider the joint effect of tuning r by increasing k and reducing δt , ensuring that r increases but not to an arbitrarily large value, so as to preserve reachability precision. \diamond

So far, we have demonstrated that the control input can be determined at τ_n to satisfy the requirement in Lemma 4.2 by searching over \mathcal{U} . However, the dynamic learning procedure, as demonstrated in Section IV-B, only permits the use of a subset of $\mathcal{U}_{n,\lambda}$ and achieves an approximation of the velocity. Therefore, we need to take the approximation error into account. Recall Definition 4.1 and $\tilde{v}_{\mathbf{x}_{n+1}}(u_{n,\lambda})$ in Section IV-B. Define $\dot{d}_{z_n}(n, \lambda) := 2\langle \mathbf{x}_n - z_n, \tilde{v}_{\mathbf{x}_{n+1}}(u_{n,\lambda}) \rangle$. We then look at the following slight modification of [22, Theorem 9].

Theorem 4.7: For a fixed $n \geq 1$, we have $\left| \min_{\lambda \in \Lambda} \dot{d}_{z_n}(n, \lambda) - \min_{\mathbf{u}(\tau_n) \in \mathcal{U}} \dot{d}_{z_n}(\phi_{\mathbf{u}}(\tau_n)) \right| \leq 2\mathcal{E}_\mu(\delta t, \epsilon)$, where $\mathcal{E}_\mu(\delta t, \epsilon) = (3L_d(C_4/C_3)\mathcal{E}_\lambda(\delta t, \epsilon) + L_dC_0\delta t)/2$; L_d is the Lipschitz constant of d_{z_n} ; $C_4 = (M_0 + 1)(L_{\max} + 1)(m + 1)^3$. \diamond

Considering the sub-optimality using $\lambda \in \Lambda$ and hence $\mathcal{U}_{n,\lambda}$, we have the following guarantee. We omit the proof due to the similarities to the proof of Theorem 4.5.

Corollary 4.8: Recall the error terms C_r and C_n in Theorem 4.5. Suppose that $\mathcal{E}_n(\delta t, \epsilon) + \mathcal{E}_\mu(\delta t, \epsilon) \leq r(b - c|\mathbf{x}_n| - \mathcal{E}_r(\delta t, \epsilon) + \epsilon M_0)$. Let $\lambda^* = \operatorname{argmin}_{\lambda \in \Lambda} \dot{d}_{z_n}(n, \lambda)$ and $\mathbf{u}(\tau_n) = u_{n,0} := (1 - \epsilon) \sum_{j \in \mathcal{I}} \lambda_j^* u_{n-1,j}$ be the controller at τ_n . Then $\dot{d}_{z_n}(\phi_{\mathbf{u}}(t)) < 0$ for all $t \in [\tau_n, \tau_{n+1})$. \diamond

D. Summary of Algorithm

Recall notation a , b and c in (3), as well as ρ and Δ_a in Section III-B. For $a \neq 0$ but with a small norm relative to b (or small Δ_a) as illustrated by [2, Section V.C], the GRS prediction maintains reasonable accuracy over a longer time horizon. In this scenario, the control synthesis technique and principle stated in Section IV-C remain the same but require the following slightly modified sufficient conditions for determining the parameters. (i) In selecting $r = r(k, \delta t)$, we follow Lemma 4.3 under the conditions

$$\epsilon > (C_3/C)\delta t; \quad \frac{2kb\tau}{b - c\rho} < T; \quad k > \frac{Cb}{b - c\rho} + \Delta_a, \quad (6)$$

which are the same as in the original case except for the last one. (ii) To maintain $\dot{d}_{z_n}(\phi_{\mathbf{u}}(t)) < 0$ for all $t \in [\tau_n, \tau_{n+1})$ for each $n \geq 1$, we follow Corollary 4.8 and choose the same controller as stated therein, but under a modified condition

$$\mathcal{E}_n(\delta t, \epsilon) + \mathcal{E}_\mu(\delta t, \epsilon) \leq r(b - c\rho - |a| - \mathcal{E}_r(\delta t, \epsilon) + \epsilon M_0). \quad (7)$$

The proofs follow exactly the same procedure as the corresponding statements we modify from, and is therefore omitted due to repetition. The condition suggests that the value of a does not alter the direction of attraction. We summarize the algorithm for in Algorithm 1.

Proposition 4.9: Following Algorithm 1, $\phi_{\mathbf{u}}$ will eventually reach $\mathcal{B}^d(y; 2r)$. \diamond

Algorithm 1 Control Synthesis

Require: $d, m, x_{0,0} := x_0, T, y \in \partial \hat{\mathcal{R}}_{\text{pse}}^T(x_0)$, and $u_{0,0} = (1 - \epsilon) \frac{G(x_0)^\dagger(y - x_0)}{\|G(x_0)^\dagger\| \|y - x_0\|}$.

Require: $x_0 = 0$; and $\delta t, \epsilon, k$ based on the conditions in (6) and (7), where $r = \sup_{\{\hat{u} \equiv \hat{u} \in \hat{\mathcal{U}}\}} |\phi_{\mathbf{u}}(k(m + 1)\delta t, x_0)|$

```

1:  $n = 0$ .
2: repeat
3:    $\tau_n = n(m + 1)\delta t$ .
4:   for  $j$  from 0 to  $m$  do
5:      $\mathbf{u}(t) \equiv u_{n,j}$  for all  $t \in [\tau_n + j\delta t, \tau_n + (j + 1)\delta t)$ 
     based on Eq. (4);
6:      $x_{n,j+1} = \phi_{\mathbf{u}}(\delta t, x_{n,j})$ .
7:   end for
8:    $\mathbf{x}_{n+1} = x_{n,m+1}$ .
9:   Determine  $z_{n+1}$  based on Lemma 4.2.
10:  Let  $u_{n+1,0} = (1 - \epsilon) \operatorname{argmin}_{\lambda \in \Lambda} \langle 2\langle \mathbf{x}_{n+1} - z_{n+1}, \sum_{j \in \mathcal{I}} \lambda_j (x_{n,j+1} - x_{n,j}) \rangle \rangle$ , where  $\sum_{j \in \mathcal{I}} \lambda_j = 1$  and  $\Lambda$  are defined in Definition 4.1.
11:   $n := n + 1$ .
12: until  $|z_n - y| < r$ .

```

Note that (6) and (7) provide theoretical guidance for parameter tuning to make Algorithm IV-D work. All perturbation terms in (7) depend only on $\delta t, \epsilon$, and k , and are either linear in ϵ and δt , or arise from \mathcal{E}_λ [22, Theorem 5], which originates from the conservative estimation in [22, Theorem 4]. These terms can be made arbitrarily small under the restrictions of (6). Although the theoretical effectiveness of Algorithm IV-D can be guaranteed over a short time span for each learning cycle, [22, Theorems 4–5] can be relaxed to reduce the restrictiveness of parameter tuning and better accommodate practical use, which is of interest for future research.

V. CASE STUDY

We use a control system with decoupled quadrotor dynamics to illustrate the proposed control synthesis algorithm, building on the same example discussed in [2, Section V.C]. We examine the scenario where a UAV collides with an obstacle, leading to undesired velocity rotations [30], [31]. To support more complex tasks, such as safe landing, it is essential to determine a reachable set of pitch and roll velocities, denoted as p and q respectively, whilst synthesizing control inputs that lead to specified pitch and roll velocities without prior knowledge of the system's dynamics.

We focus on the situation where the inertia in the x - and y -axes are identical, allowing the yaw rate to be directly altered by increasing the corresponding torque action without impacting p and q . To simplify the problem, we trivially reduce the yaw state to be constant $\pi/2$.

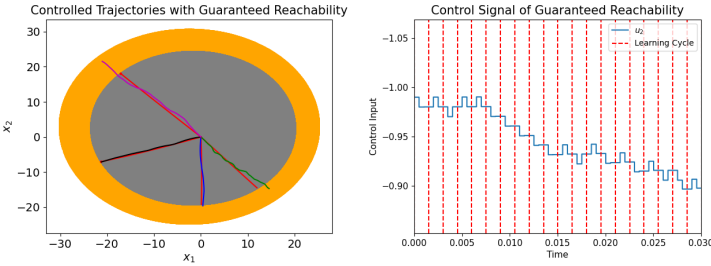


Fig. 2. (l.h.s.) Controlled trajectories for Scenario A-D. The grey region represents the GRS; the orange region indicates the true reachable set; the controlled trajectories for A-D, respectively, are shown in black, blue, green, and purple; the red trajectories represent the proxy controlled paths to four randomly sampled points on the boundary of the GRS for the true system aims to track. (r.h.s.) Selected partial control signals for Scenario B.

To apply the proposed algorithm, we let the initial conditions after collision be $(p_0, q_0) = (15, 10)$ radians per second, and then perform a coordinate transformation by introducing $x_1 = p - 15$ and $x_2 = q - 10$. The recast system is as follows.

$$\frac{d}{dt} \begin{bmatrix} x_1(t) \\ x_2(t) \end{bmatrix} = \begin{bmatrix} \frac{\pi(J_y - J_z)}{2J_x} (x_2(t) + 10) \\ \frac{\pi(J_z - J_x)}{2J_y} (x_1(t) + 15) \end{bmatrix} + \begin{bmatrix} \frac{1}{J_x} \tau_\phi \\ \frac{1}{J_y} \tau_\theta \end{bmatrix}, \quad (8)$$

with initial conditions $x(0) := (x_1(0), x_2(0)) = (0, 0)$ and torque inputs $(u_1, u_2) := (\tau_\phi, \tau_\theta) \in \mathcal{B}^2(0; 1)$ for the roll and pitch. We also set $J_x = \frac{2MR^2}{5} + 2l^2m$, $J_y = J_x$, $J_z = \frac{2MR^2}{5} + 4l^2m$, where $M = 1\text{kg}$ and $R = 0.1\text{m}$ represent the mass and radius of the central frame. The central frame is connected to four point masses $m = 0.1\text{kg}$, each representing one of the four propellers, positioned at an equidistant length of $l = 0.5\text{m}$ from the central sphere. Consequently, $a \approx (-8.73, 13.09)^\top$, and $b = \|G(0)^\dagger\|^{-1} \approx 111.11$. We also derive a conservative Lipschitz bounds to be $L_f = L_G = 1$, and therefore, $L_0 = 1$, and $\mathbb{B} = \mathcal{B}^2(f(0); 111.11 - 2|x|)$ for the domain where (3) is well defined.

Remark 5.1: Note that while the true system dynamics are described in (8), they are unknown to the controller. The controller only has access to the trajectory data and the parameters required in Algorithm 1. Hence, the choice of model does not affect the proposed control technique. Without real data, we can only leverage numerical ODE solvers based on the exact model (8) to generate trajectory data. One can also randomly choose the aforementioned coefficients in (8); regardless, we only need an estimation of the parameters as mentioned in Section III-A for GRS evaluation and subsequent control synthesis. We would also like to refer readers interested in other simulations to https://github.com/TahaShafa/reachable_predictive_control, which includes video visualizations. \diamond

In the simulation, we aim to reach a neighborhood of any point on the boundary of the underestimated GRS for $T = 0.25$. To succinctly represent and demonstrate the effectiveness of the proposed algorithm, we test it across four scenarios with different settings of the parameters $(\delta t, \epsilon, k)$ and display the controlled paths in a single picture. Since the theoretical result on the guaranteed accuracy does not distinguish between target points, we randomly sample points on

the boundary of the GRS. Detailed settings for $(\delta t, \epsilon, k)$ are A: $(0.0001, 0.005, 5)$; B: $(0.0005, 0.01, 6)$; C: $(0.0008, 0.08, 12)$; D: $(0.0015, 0.10, 40)$. The theoretical accuracy, indicated by r , can be computed based on the chosen parameters and is equal to 0.18, 1.11, 3.48, 18.83 for the four cases, respectively.

The controlled trajectories for A-D are presented as shown in Figure 2. We choose to present only a zoomed-in view of the control signal for Scenario B to demonstrate the piecewise constant shape resulting from a short period of the learning cycle. The accuracy across scenarios A-D decreases as predicted. Specifically, Scenario A closely adheres to the trackable path, while D significantly deviates from the intended trackable path. As depicted in the r.h.s. picture of Figure 2, there are three sub-intervals within each learning cycle n , corresponding to $u_{n,j}$ for $j = 0, 1, 2$.

VI. CONCLUSION

In this paper, we investigate the control properties of an underapproximated control system, whose reachable set represents a guaranteed reachable set of the true but unknown system. Then, we utilize the connection between this proxy system and the true system to synthesize controllers that guide the trajectory to reach a neighborhood of a specified point within the guaranteed reachable set. The essence of the proposed method is to automatically generate a sequence of points $\{z_n\}$, converging to the required reachable point y , for the true trajectory to follow. This approach allows the use of historical data within a learning cycle to determine the trajectory's direction for the subsequent learning cycle.

We also explore the sufficient conditions for the controlled trajectory to approach each z_n within every learning cycle, ensuring it will eventually reach a small neighborhood of the specified point y . It would be of significant engineering interest to improve the error estimation and tune the parameters, as outlined in Algorithm 1, to automate the learning and control of an unknown system based on a single trajectory run.

For future work, building on the connections between [2] and the recent work [26] on extending GRS evaluation to Riemannian manifolds, the proposed method in this study provides a foundation for controlling unknown systems under more relaxed assumptions, with applications to underactuated systems. Additionally, exploring how to control an unknown system to reach a region beyond the current short-time-frame estimation of the GRS is crucial. This may involve online waypoint generation and adaptive control guided by iterative application of our current methods. As data accumulates through this process, recent advances in Koopman-based system identification [14], [15] can be leveraged for more precise dynamics learning. Robust control methods can then be employed to address the remaining control tasks with better performance, ultimately achieving resilience and guaranteed task completion for unknown nonlinear control systems.

REFERENCES

- [1] T. Shafa and M. Ornik, "Maximal ellipsoid method for guaranteed reachability of unknown fully actuated systems," in *IEEE Conference on Decision and Control (CDC)*, pp. 5002–5007, IEEE, 2022.

- [2] T. Shafa and M. Ornik, "Reachability of nonlinear systems with unknown dynamics," *IEEE Transactions on Automatic Control*, vol. 68, no. 4, pp. 2407–2414, 2023.
- [3] L. Cheng, Z. Wang, F. Jiang, and J. Li, "Adaptive neural network control of nonlinear systems with unknown dynamics," *Advances in Space Research*, vol. 67, no. 3, pp. 1114–1123, 2021.
- [4] G. Bianchin, M. Vaquero, J. Cortés, and E. Dall'Anese, "Data-driven synthesis of optimization-based controllers for regulation of unknown linear systems," in *2021 60th IEEE Conference on Decision and Control (CDC)*, pp. 5783–5788, 2021.
- [5] A. J. Taylor, V. D. Dorobantu, S. Dean, B. Recht, Y. Yue, and A. D. Ames, "Towards robust data-driven control synthesis for nonlinear systems with actuation uncertainty," in *2021 60th IEEE Conference on Decision and Control (CDC)*, pp. 6469–6476, 2021.
- [6] H. V. A. Truong, M. H. Nguyen, D. T. Tran, and K. K. Ahn, "A novel adaptive neural network-based time-delayed estimation control for nonlinear systems subject to disturbances and unknown dynamics," *ISA Transactions*, vol. 142, pp. 214–227, 2023.
- [7] A. U. Awan and M. Zamani, "Formal synthesis of safety controllers for unknown systems using Gaussian process transfer learning," *IEEE Control Systems Letters*, 2023.
- [8] J. Kocijan, R. Murray-Smith, C. E. Rasmussen, and A. Girard, "Gaussian process model based predictive control," in *Proceedings of the 2004 American control conference*, vol. 3, pp. 2214–2219, 2004.
- [9] R. Chen, X. Jin, S. Laima, Y. Huang, and H. Li, "Intelligent modeling of nonlinear dynamical systems by machine learning," *International Journal of Non-Linear Mechanics*, vol. 142, p. 103984, 2022.
- [10] L. Jin, Z. Liu, and L. Li, "Prediction and identification of nonlinear dynamical systems using machine learning approaches," *Journal of Industrial Information Integration*, vol. 35, p. 100503, 2023.
- [11] A. Mauroy and J. Goncalves, "Koopman-based lifting techniques for nonlinear systems identification," *IEEE Transactions on Automatic Control*, vol. 65, no. 6, pp. 2550–2565, 2019.
- [12] Z. Zeng, Z. Yue, A. Mauroy, J. Goncalves, and Y. Yuan, "A sampling theorem for exact identification of continuous-time nonlinear dynamical systems," in *2022 IEEE 61st Conference on Decision and Control (CDC)*, pp. 6686–6692, 2022.
- [13] Y. Meng, R. Zhou, and J. Liu, "Learning regions of attraction in unknown dynamical systems via zubov-koopman lifting: Regularities and convergence," *IEEE Transactions on Automatic Control*, 2025.
- [14] Y. Meng, R. Zhou, M. Ornik, and J. Liu, "Resolvent-type data-driven learning of generators for unknown continuous-time dynamical systems," *arXiv preprint arXiv:2411.00923*, 2024.
- [15] Z. Zeng, R. Zhou, Y. Meng, and J. Liu, "Data-driven optimal control of unknown nonlinear dynamical systems using the koopman operator," in *Annual Learning for Dynamics & Control Conference*, pp. 1127–1139, 2025.
- [16] E. Shmalko and A. Diveev, "Control synthesis as machine learning control by symbolic regression methods," *Applied Sciences*, vol. 11, no. 12, p. 5468, 2021.
- [17] Y. Meng, R. Zhou, A. Mukherjee, M. Fitzsimmons, C. Song, and J. Liu, "Physics-informed neural network policy iteration: Algorithms, convergence, and verification," in *International Conference on Machine Learning*, pp. 35378–35403, 2024.
- [18] A. D. Ames, S. Coogan, M. Egerstedt, G. Notomista, K. Sreenath, and P. Tabuada, "Control barrier functions: Theory and applications," in *2019 18th European control conference (ECC)*, pp. 3420–3431, IEEE, 2019.
- [19] D. Seto, A. M. Annaswamy, and J. Baillieul, "Adaptive control of nonlinear systems with a triangular structure," *IEEE Transactions on Automatic Control*, vol. 39, no. 7, pp. 1411–1428, 1994.
- [20] Z.-P. Jiang and L. Praly, "Design of robust adaptive controllers for nonlinear systems with dynamic uncertainties," *Automatica*, vol. 34, no. 7, pp. 825–840, 1998.
- [21] A. Astolfi, D. Karagiannis, and R. Ortega, *Nonlinear and Adaptive Control with Applications*, vol. 187. Springer, 2008.
- [22] M. Ornik, S. Carr, A. Israel, and U. Topcu, "Control-oriented learning on the fly," *IEEE Transactions on Automatic Control*, vol. 65, no. 11, pp. 4800–4807, 2019.
- [23] M. Margaliot, "On the reachable set of nonlinear control systems with a nilpotent lie algebra," in *2007 European Control Conference (ECC)*, pp. 4261–4267, 2007.
- [24] R. Vinter, "A characterization of the reachable set for nonlinear control systems," *SIAM Journal on Control and Optimization*, vol. 18, no. 6, pp. 599–610, 1980.
- [25] H. El-Kebir, A. Piroshmanishvili, and M. Ornik, "Online guaranteed reachable set approximation for systems with changed dynamics and control authority," *IEEE Transactions on Automatic Control*, 2023.
- [26] T. Shafa and M. Ornik, "Guaranteed reachability on Riemannian manifolds for unknown nonlinear systems," *arXiv preprint arXiv:2404.09850*, 2024.
- [27] M. Rungger and M. Zamani, "Accurate reachability analysis of uncertain nonlinear systems," in *Proceedings of the 21st international conference on hybrid systems: Computation and control*, pp. 61–70, 2018.
- [28] N. Ramdani and N. S. Nedialkov, "Computing reachable sets for uncertain nonlinear hybrid systems using interval constraint-propagation techniques," *Nonlinear Analysis: Hybrid Systems*, vol. 5, no. 2, pp. 149–162, 2011.
- [29] Z. Han and B. H. Krogh, "Reachability analysis of nonlinear systems using trajectory piecewise linearized models," in *2006 American Control Conference*, pp. 6–pp, IEEE, 2006.
- [30] G. Chowdhary, E. N. Johnson, R. Chandramohan, M. S. Kimbrell, and A. Calise, "Guidance and control of airplanes under actuator failures and severe structural damage," *Journal of Guidance, Control, and Dynamics*, vol. 36, no. 4, pp. 1093–1104, 2013.
- [31] D. Jourdan, M. Piedmonte, V. Gavrillets, D. Vos, and J. McCormick, "Enhancing UAV survivability through damage tolerant control," in *AIAA Guidance, Navigation, and Control Conference*, pp. 7548–7573, 2010.
- [32] H. K. Khalil, *Nonlinear systems*, vol. 3.
- [33] S. P. Boyd and L. Vandenberghe, *Convex optimization*. Cambridge university press, 2004.
- [34] R. Tyrrell Rockafellar, "Convex analysis," *Princeton mathematical series*, vol. 28, 1970.

APPENDIX A PROOFS IN SECTION III

Proof of Proposition 3.2: We assume the contrary, as specified in the statement, then, there exists a $\hat{\mathbf{u}}$ and a $t \in [0, T)$ such that $\hat{\phi}_{\hat{\mathbf{u}}}(t) = y \in \partial \hat{\mathcal{R}}^{\leq T}(x_0)$. Then, $\hat{\phi}_{\hat{\mathbf{u}}}(T) = y + a(T - t) + \int_t^T (b - c|\hat{\phi}_{\hat{\mathbf{u}}}(s)|)\hat{\mathbf{u}}(s) ds$. Since $\hat{\mathcal{U}}$ is compact, convex, and centered at 0, for any $s \in [t, T)$, we can find a $\hat{\mathbf{u}}(s)$ such that $\hat{\mathbf{u}}(s) = \frac{k(s)(y - x_0) - a}{b - c|\hat{\phi}_{\hat{\mathbf{u}}}(s)|}$, where $k(s)$ is some positive number. By assumption, it can be verified that $\hat{\mathbf{u}}(s) \in \hat{\mathcal{U}}$ for all $s \in [t, T)$. Therefore, $\hat{\phi}_{\hat{\mathbf{u}}}(T) = y + a(T - t) + (y - x_0) \int_t^T k(s) ds - \int_t^T a ds = y + (y - x_0) \int_t^T k(s) ds$. Let $\lambda := 1 + \int_t^T k(s) > 1$, then $\hat{\phi}_{\hat{\mathbf{u}}}(T) = \lambda(y) + (1 - \lambda)x_0$. Since $y \in \partial \hat{\mathcal{R}}^{\leq T}(x_0)$ and $x_0 \in \text{Int}(\hat{\mathcal{R}}^{\leq T}(x_0))$, the point $\hat{\phi}_{\hat{\mathbf{u}}}(T)$ is located on the line extending from x_0 through y , and continues beyond y , in the direction from x_0 to y . Due to the convexity property of $\hat{\mathcal{R}}^{\leq T}(x_0)$ as stated in [2, Section III], and the above construction of the signal used to extend the trajectory outward from x_0 to y , we have that $\hat{\phi}_{\hat{\mathbf{u}}}(T) \notin \hat{\mathcal{R}}^{\leq T}(x_0)$, which violates the assumption. We hence prove the statement. ■

Proof of Proposition 3.3: Consider any $y \in \partial \hat{\mathcal{R}}^T(x_0)$ and $\nu = \frac{y}{|y|} \in \partial \hat{\mathcal{U}}$. For any $\hat{\mathbf{u}}$, define $\rho(t) = \langle \hat{\phi}_{\hat{\mathbf{u}}}(t), \nu \rangle$. Then, $\dot{\rho}(t) = (b - c|\hat{\phi}_{\hat{\mathbf{u}}}(t)|)\langle \hat{\mathbf{u}}(t), \nu \rangle$. Since $\rho(t) \leq |\hat{\phi}_{\hat{\mathbf{u}}}(t)|$ and $\langle \hat{\mathbf{u}}(t), \nu \rangle \leq |\hat{\mathbf{u}}(t)||\nu| = 1$, we have $\dot{\rho}(t) \leq b - c\rho(t)$. On the other hand, let $\hat{\mathbf{u}}^* \equiv \nu$. Then, $\hat{\phi}_{\hat{\mathbf{u}}^*}(t) = \nu \int_0^t (b - c|\hat{\phi}_{\hat{\mathbf{u}}^*}(s)|) ds$ is in the same direction as ν . Consider $\rho^*(t) = \langle \hat{\phi}_{\hat{\mathbf{u}}^*}(t), \nu \rangle$, then $\dot{\rho}^*(t) = (b - c|\hat{\phi}_{\hat{\mathbf{u}}^*}(t)|)\langle \nu, \nu \rangle = b - c\rho^*(t)$. By the *Comparison Principle* [32, Lemma 3.4], we have $\langle \hat{\phi}_{\hat{\mathbf{u}}}(T), \nu \rangle \leq \langle \hat{\phi}_{\hat{\mathbf{u}}^*}(T), \nu \rangle$, which indicates that $\hat{\phi}_{\hat{\mathbf{u}}^*}(T) \in \partial \hat{\mathcal{R}}^T(x_0)$ according to the supporting hyperplane theorem [33]. Additionally, by [2, Corollary 3], $\hat{\phi}_{\hat{\mathbf{u}}^*}(T)$ can only be y . The above indicates that $\partial \hat{\mathcal{R}}^T(x_0) \subseteq \partial \hat{\mathcal{R}}_{\text{pse}}^T(x_0)$. By the fact that $\hat{\mathcal{R}}^T(x_0)$ is convex and $\partial \hat{\mathcal{R}}_{\text{pse}}^T(x_0) \subseteq \hat{\mathcal{R}}^T(x_0)$, we obtain $\partial \hat{\mathcal{R}}_{\text{pse}}^T(x_0) \subseteq \partial \hat{\mathcal{R}}^T(x_0)$ [34], which proves the first part of the conclusion.

The second part follows immediately. \blacksquare

Proof of Proposition 3.4: Let $\eta(t) = \hat{\phi}_{\hat{\mathbf{u}}}(t) - at$, then η solves $\dot{\eta}(t) = (b - c|\eta(t) + at|)\hat{\mathbf{u}}(t)$. We have $\vartheta_a(t) := \eta(t) - \bar{\phi}_{\hat{\mathbf{u}}}(t)$. Then, $\dot{\vartheta}_a(t) = (b - c|\eta(t) + at|)\hat{\mathbf{u}}(t) - (b - c|\eta(t)|)\hat{\mathbf{u}}(t) + (b - c|\eta(t)|)\hat{\mathbf{u}}(t) - (b - c|\bar{\phi}_{\hat{\mathbf{u}}}(t)|)\hat{\mathbf{u}}(t)$. Consequently, for $\vartheta_a(t) \neq 0$,

$$\begin{aligned} \frac{d}{dt}|\vartheta_a(t)| &= \vartheta_a(t) \cdot \dot{\vartheta}_a(t)/|\vartheta_a(t)| \leq |\dot{\vartheta}_a(t)| \\ &\leq c|\eta(t) + at| - |\eta(t)| + c|\eta(t)| - |\bar{\phi}_{\hat{\mathbf{u}}}(t)| \\ &\leq c|a|t + c|\vartheta_a(t)|, \end{aligned}$$

and $d(e^{-ct}|\vartheta_a(t)|)/dt \leq -ce^{-ct}|\vartheta_a(t)| + c|a|te^{-ct} + ce^{-ct}|\vartheta_a(t)| \leq c|a|te^{-ct}$. Then, $e^{-ct}|\vartheta_a(t)| \leq c|a|\int_0^t se^{-cs}ds$, and the conclusion follows. \blacksquare

APPENDIX B PROOFS IN SECTION IV

Proof of Lemma 4.2: Note that $\mathbf{x}_{n+1} = \phi_{\mathbf{u}}(\tau_{n+1})$. Given the assumptions that $\dot{d}_{z_n}(\phi_{\mathbf{u}}(t)) < 0$ for all $t \in [\tau_n, \tau_{n+1})$, it is clear that $|\mathbf{x}_{n+1} - z_n| < r$. To determine z_{n+1} , one needs to solve the equation $|z_{n+1} - \mathbf{x}_{n+1}|^2 = r^2$ with $z_{n+1} = \theta_{n+1}y$. Since $|\mathbf{x}_{n+1} - z_n| < r$, it can be guaranteed that there exists at least one solution such that $\theta_{n+1} > \theta_n$. Thus, the first part of the statement holds. It is also clear that $r - |\mathbf{x}_{n+1} - z_n| \leq |z_{n+1} - z_n| \leq r + |\mathbf{x}_{n+1} - z_n| < 2r$, which completes the proof. \blacksquare

Proof of Lemma 4.3: Recall the notation $\tau := (m + 1)\delta t$. For $\delta t > 0$ arbitrarily small, we have

$$\begin{aligned} \phi_{\mathbf{u}}(\tau, x_0) &= \sum_{j \in \mathcal{I}} \int_{j\delta t}^{(j+1)\delta t} (f(x_0) + G(x_0)u_{0,j})ds + \mathcal{O}(\delta t^2) \\ &= \delta t \cdot \left(\sum_{j \in \mathcal{I}} G(x_0)u_{0,j} \right) + \mathcal{O}(\delta t^2) \\ &= \tau \cdot (G(x_0)u_{0,0}) + \sum_{j \in \mathcal{I}_0} \delta t \cdot \epsilon G(x_0)\mathbf{e}_j + \mathcal{O}(\delta t^2), \end{aligned} \quad (9)$$

where $|\mathcal{O}(\delta t^2)| \leq \int_0^\tau \|f(\phi_{\mathbf{u}}(t)) - f(x_0)\| + \|G(\phi_{\mathbf{u}}(t)) - G(x_0)\| dt \leq \int_0^\tau 2L_0C_0t dt = L_0M_0(m+1)^3\delta t^2 = C_3 \cdot \delta t^2$ [22, Lemma 4]. In addition, by the construction of $u_{0,0}$, we have $\tau \cdot (G(x_0)u_{0,0}) = \tau(1 - \epsilon)G(x_0)G(x_0)^\dagger \frac{by}{|y|}$. Define $\underline{r} := k\tau(b - c\rho)$. We then have

$$\begin{aligned} |\phi_{\mathbf{u}}(\tau, x_0)| &\leq |\tau(1 - \epsilon)\frac{Cby}{|y|}| + \left| \sum_{j \in \mathcal{I}_0} \delta t \cdot \epsilon G(x_0)\mathbf{e}_j \right| + |\mathcal{O}(\delta t^2)| \\ &\leq C\tau(1 - \epsilon)b + m \cdot \delta t \cdot \epsilon \cdot \|G(x_0)\| + |\mathcal{O}(\delta t^2)| \\ &= C\tau(1 - \epsilon)b + C\tau \cdot \epsilon b - C\epsilon\delta t + |\mathcal{O}(\delta t^2)| \\ &\leq \underline{r} + (Cb\tau - \underline{r}) - C\epsilon\delta t + C_3\delta t^2 \\ &< \underline{r} + (Cb\tau - \underline{r}), \end{aligned} \quad (10)$$

where, in the last inequality, $r \geq |\hat{\phi}_{\hat{\mathbf{u}}}(k\tau, x_0)| = \int_0^{k\tau} (b - c|\hat{\phi}_{\hat{\mathbf{u}}}(t, x_0)|)dt > \underline{r}$ holds under all $\hat{\mathbf{u}} = \hat{u} \in \partial\hat{\mathcal{U}}$, and $-C\epsilon\delta t + C_3\delta t^2$ is canceled due to the additional assumption on its sign given in the statement. Note that for k such that $k > Cb/(b - c\rho)$, it follows from (10) that $|\phi_{\mathbf{u}}(\tau, x_0)| < r$.

Additionally, for sufficiently small δt and $T > \frac{2kb\tau}{b - c\rho}$, we have $2r < 2\int_0^{k\tau} (b - 0)dt < (b - c\rho)T < |y|$. By solving $(z_1 - \phi_{\mathbf{u}}(\tau))^2 = r^2$ with $z_1 = \theta_1 y$ and $\theta_1 \in (0, 1)$, the claim in the statement follows immediately as $|\phi_{\mathbf{u}}(\tau) - z_0| < r$ for $z_0 = 0$ and $|z_1 - z_0| < 2r < |y|$. \blacksquare

Proof of Proposition 4.4:

Note that, for each $n \geq 1$, $\hat{\phi}_{\hat{\mathbf{u}}}(t, \mathbf{x}_n)$ lies on the line extending from \mathbf{x}_n through z_n and moves toward z_n , under the control $\hat{\mathbf{u}}(t) = \frac{z_n - \mathbf{x}_n}{|z_n - \mathbf{x}_n|}$ before reaching z_n . We also have the instantaneous Lie derivative along the path of $\hat{\phi}_{\hat{\mathbf{u}}}(t, \mathbf{x}_n)$ at $t = 0$ as $\dot{d}_{z_n}(\hat{\phi}_{\hat{\mathbf{u}}}(0, \mathbf{x}_n)) = \langle \nabla d_{z_n}(\hat{\phi}_{\hat{\mathbf{u}}}(0, \mathbf{x}_n)), (b - c|\hat{\phi}_{\hat{\mathbf{u}}}(0, \mathbf{x}_n)|)\hat{\mathbf{u}}(0) \rangle = \langle 2(\mathbf{x}_n - z_n), (b - c|\mathbf{x}_n|)\hat{\mathbf{u}}(0) \rangle = -2r(b - c|\mathbf{x}_n|)$

Recall $\phi_{\mathbf{u}}(\tau_n, x_0) = \mathbf{x}_n$. By Theorem 3.1, there exists a \tilde{u} such that $f(\mathbf{x}_n) + G(\mathbf{x}_n)\tilde{u} = (b - c|\mathbf{x}_n|)\hat{\mathbf{u}}(0)$. Then, $\langle \nabla d_{z_n}(\mathbf{x}_n), f(\mathbf{x}_n) + G(\mathbf{x}_n)\tilde{u} \rangle = -2r(b - c|\mathbf{x}_n|)$. Therefore, $\min_{u \in \mathcal{U}} \langle \nabla d_{z_n}(\mathbf{x}_n), f(\mathbf{x}_n) + G(\mathbf{x}_n)u \rangle \leq -2r(b - c|\mathbf{x}_n|)$. The optimal input $\arg\min_{u \in \mathcal{U}} \langle \nabla d_{z_n}(\mathbf{x}_n), f(\mathbf{x}_n) + G(\mathbf{x}_n)u \rangle$ satisfies the property in the statement. \blacksquare

Proof of Theorem 4.5: Let n be fixed. For simplicity, we use the shorthand notation $\mathbf{x}(t) := \phi_{\mathbf{u}}(t, x_0)$ for any $t \in [\tau_n, \tau_{n+1})$. Let $v(\mathbf{x}(t)) := f(\mathbf{x}(t)) + G(\mathbf{x}(t))\mathbf{u}(t)$, $v(\mathbf{x}_n) := f(\mathbf{x}_n) + G(\mathbf{x}_n)\mathbf{u}(\tau_n)$. Then, $|v(\mathbf{x}(t)) - v(\mathbf{x}_n)| \leq |f(\mathbf{x}(t)) - f(\mathbf{x}_n)| + |G(\mathbf{x}(t))\mathbf{u}(\tau_n) - G(\mathbf{x}_n)\mathbf{u}(\tau_n) + G(\mathbf{x}(t))(\mathbf{u}(t) - \mathbf{u}(\tau_n))| \leq 2L_0C_0(t - \tau_n) + \epsilon M_0$, and

$$\begin{aligned} &\langle (\mathbf{x}(t) - z_n), v(\mathbf{x}(t)) \rangle \\ &= \langle \mathbf{x}_n - z_n, v(\mathbf{x}_n) \rangle + \langle \mathbf{x}(t) - \mathbf{x}_n, v(\mathbf{x}_n) \rangle \\ &\quad + \langle \mathbf{x}(t) - \mathbf{x}_n, v(\mathbf{x}(t)) - v(\mathbf{x}_n) \rangle + \langle \mathbf{x}_n - z_n, v(\mathbf{x}(t)) - v(\mathbf{x}_n) \rangle \\ &\leq -r(b - c|\mathbf{x}_n|) + 2M_0|\mathbf{x}(t) - \mathbf{x}_n| \\ &\quad + |\mathbf{x}(t) - \mathbf{x}_n| |v(\mathbf{x}(t)) - v(\mathbf{x}_n)| + r|v(\mathbf{x}(t)) - v(\mathbf{x}_n)| \\ &\leq -r(b - c|\mathbf{x}_n|) + 2M_0C_0(t - \tau_n) \\ &\quad + (C_0(t - \tau_n) + r) \cdot (2L_0C_0(t - \tau_n) + \epsilon M_0) \\ &< -r(b - c|\mathbf{x}_n|) + 2M_0C_1\delta t + (C_1\delta t + r) \cdot (C_2\delta t + \epsilon M_0) \\ &= -r(b - c|\mathbf{x}_n|) + r \cdot \mathcal{E}_r(\delta t, \epsilon) + \mathcal{E}_n(\delta t, \epsilon) \end{aligned} \quad (11)$$

The conclusion follows by the assumption. \blacksquare

Proof of Proposition 4.9: Recall (7) and let $\Gamma = \mathcal{E}_n(\delta t, \epsilon) + \mathcal{E}_\mu(\delta t, \epsilon) - r(b - c|\mathbf{x}_n| - |a| - \mathcal{E}_r(\delta t, \epsilon) + \epsilon M_0)$. Consider $\Delta_1 := (2M_0C_0 + 2rL_0C_0 + \epsilon M_0)$ and $\Delta_2(t) := 2rL_0C_0$. Then, for each n and for $t \in [\tau_n, \tau_{n+1})$, by a similar argument in Theorem 4.5, we have $\frac{1}{2}\dot{d}_{z_n}(\phi_{\mathbf{u}}(t)) \leq \Gamma - \Delta_1 \cdot (\tau_{n+1} - t) - \Delta_2 \cdot (\tau^2 - (t - \tau_n)^2) < \Gamma \leq 0$. Therefore, $d_{z_n}(\phi_{\mathbf{u}}(\tau_{n+1})) - d_{z_n}(\phi_{\mathbf{u}}(\tau_n)) \leq 2\int_{\tau_n}^{\tau_{n+1}} [\Gamma - \Delta_1 \cdot (\tau_{n+1} - t) - \Delta_2 \cdot (\tau^2 - (t - \tau_n)^2)] dt = 2\Gamma\tau - \Delta_1\tau^2 - \frac{2}{3}\Delta_2\tau^3$. Since $\Gamma \leq 0$, we have $d_{z_n}(\phi_{\mathbf{u}}(\tau_{n+1})) - d_{z_n}(\phi_{\mathbf{u}}(\tau_n)) = |\mathbf{x}_{n+1} - z_n|^2 - r^2 \leq -\Delta_1\tau^2 - \frac{4}{3}\Delta_2\tau^3$, implying that $r - |\mathbf{x}_{n+1} - z_n|$ has a uniform lower bound. By the construction of $\{z_n\}$ in Lemma 4.2, particularly the guarantee of incremental and uniformly minimal distance for $|z_{n+1} - z_n|$ for each n , there exists a finite N such that $N = \inf\{n \in \mathbb{N} : z_n \in \mathcal{B}^d(y; r)\}$.

By the property of the controller, specifically the attractivity to each z_n under the modified condition in (6) and (7), there exists a finite time $\tilde{T} \leq \tau_{N+1}$ such that $|\phi_{\mathbf{u}}(\tilde{T}, x_0) - z_N| < r$. The conclusion follows by the triangle inequality. \blacksquare

APPENDIX C
REACHABLE SET OF THE PROXY SYSTEM

We demonstrate that when $a \neq 0$, the property stated in Proposition 3.3 may not hold.

Proposition C.1: Given a T such that $\hat{\mathcal{R}}^{\leq T}(x_0) \subseteq \text{Int}(\mathbb{B})$. Suppose $\text{Im}(G(x_0)) = \mathbb{R}^d$. For $a \neq 0$, $\partial\hat{\mathcal{R}}_{\text{pse}}^T(x_0) \neq \partial\hat{\mathcal{R}}^T(x_0)$.

Proof: Due to the convexity of $\hat{\mathcal{R}}^T(x_0)$, the supporting hyperplane theorem [34] implies that for any non-zero $\nu \in \mathbb{R}^d$, there exists $x^* \in \partial\hat{\mathcal{R}}^T(x_0)$ such that $\langle \nu, x^* \rangle \geq \langle \nu, x \rangle$ for all $x \in \hat{\mathcal{R}}^T(x_0)$. Let $\hat{\mathbf{u}}^*$ be the control signal such that $\hat{\phi}_{\hat{\mathbf{u}}^*}(T) = x^*$, then, $\hat{\mathbf{u}}^*$ can be obtained by finding the maximizer of $\langle \nu, \hat{\phi}_{\hat{\mathbf{u}}}(T) \rangle$ subject to (3). Define the Hamiltonian $H(\hat{x}, \hat{u}, p) = \langle p, a + (b - c|\hat{x}|)\hat{u} \rangle$, where $p \in \mathbb{R}^d$ is the adjoint (co-state) vector. According to Pontryagin's maximum principle (PMP), the optimal control \hat{u}^* minimizes the Hamiltonian with respect to \hat{u} , leading to $|\hat{u}^*| = 1$ if there exists $\hat{u} \in \hat{\mathcal{U}}$ such that $\langle p, \hat{u} \rangle \neq 0$; otherwise, \hat{u}^* is set to be anything in $\hat{\mathcal{U}}$.

Particularly, if $\text{Im} G(x(0)) = \mathbb{R}^d$, $\hat{u}^* = \frac{p}{|p|}$ if $p \neq 0$, and \hat{u}^* can be arbitrary otherwise. The optimal control law is $\hat{\mathbf{u}}^*(t) = \frac{p(t)}{|p(t)|}$, where the adjoint equation is $\dot{p}(t) = \partial_{\hat{x}} H(\hat{\phi}_{\hat{\mathbf{u}}^*}(t), \hat{\mathbf{u}}^*(t), p(t)) = c \frac{|p(t)|}{|\hat{\phi}_{\hat{\mathbf{u}}^*}(t)|} \hat{\phi}_{\hat{\mathbf{u}}^*}(t)$ with $p(T) = \nu$, provided $\hat{\phi}_{\hat{\mathbf{u}}^*}(t) \neq 0$. However, under the optimal control law, the set of t for which $\hat{\phi}_{\hat{\mathbf{u}}^*}(t) \neq 0$ has measure 0, and $p(t)$ can be determined by continuity despite the singularity. Now, suppose $\hat{\mathbf{u}}^* \equiv \mathbf{e}$ is in a constant direction for some unit vector \mathbf{e} , then $p(t)$ is in a constant direction, which implies that $\hat{\phi}_{\hat{\mathbf{u}}^*}(t)$ is in the same direction. However, this further implies that $\hat{\phi}_{\hat{\mathbf{u}}^*}(t) = \rho(s)w$ for a scalar function ρ and a fixed vector $w \in \mathbb{R}^d$, which in turn requires that $a + (b - |\hat{\phi}_{\hat{\mathbf{u}}^*}(t)|)\mathbf{e}$ must always be consistent with w . This cannot hold for all \mathbf{e} , particularly when a is not parallel to \mathbf{e} , as it would additionally require $|\hat{\phi}_{\hat{\mathbf{u}}^*}(t)|$ to remain constant (an impossible condition under \mathbf{e}). Then, the above argument concludes that there exist constant control inputs $\hat{\mathbf{u}}$ with $|\hat{\mathbf{u}}| \equiv 1$ that cannot steer the trajectory to the boundary. The statement is proved. ■

The above statement suggests that the $\partial\hat{\mathcal{R}}_{\text{pse}}^T(x_0)$ may lie strictly inside the true boundary. The condition of $\partial\hat{\mathcal{R}}_{\text{pse}}^T(x_0) \neq \partial\hat{\mathcal{R}}^T(x_0)$ for the case when $\text{Im}(G(x_0)) \neq \mathbb{R}^d$ can also be shown in a similar manner to the proof of Proposition C.1. However, we omit it here as it is less relevant to our current problem.

The following statement shows how spatial scaling of $\hat{\mathcal{U}}$ is related to the effect of temporal scaling.

Corollary C.2: Suppose that T and $k > 0$ are such that $\hat{\mathcal{R}}^{\leq kT}(x_0) \subseteq \text{Int}(\mathbb{B})$ and $\hat{\mathcal{R}}^{\leq T}(x_0) \subseteq \text{Int}(\mathbb{B})$. Let z be such that $z \in \partial\hat{\mathcal{R}}^{kT}(x_0)$ for some $k > 0$. Then, there exists a $\tilde{\mathbf{u}} = k\hat{\mathbf{u}}$ such that $z \in \partial\hat{\mathcal{R}}^T(x_0)$, where $\hat{\mathcal{R}}^T(x_0)$ is the reachable set at T of system (3) under $k\hat{\mathcal{U}} := \{\tilde{\mathbf{u}} : \tilde{\mathbf{u}} = k\hat{\mathbf{u}}, \hat{\mathbf{u}} \in \hat{\mathcal{U}}\}$. ◊

Proof of Corollary C.2: By Proposition C.1, the controller $\hat{\mathbf{u}}$ is a constant vector. Note that, for each t , $\hat{\phi}_{\hat{\mathbf{u}}}(t)$ solves

$d\hat{\phi}_{\hat{\mathbf{u}}}(t)/dt = (b - c|\hat{\phi}_{\hat{\mathbf{u}}}(t)|)k\hat{\mathbf{u}}$, whereas $\hat{\phi}_{\hat{\mathbf{u}}}(kt)$ solves $d\hat{\phi}_{\hat{\mathbf{u}}}(kt)/d(kt) = (b - c|\hat{\phi}_{\hat{\mathbf{u}}}(kt, x)|)\hat{\mathbf{u}}$ in the slow time scale of kt . Then, $d\hat{\phi}_{\hat{\mathbf{u}}}(kt)/dt = (b - c|\hat{\phi}_{\hat{\mathbf{u}}}(kt)|)k\hat{\mathbf{u}}$, which implies that $\hat{\phi}_{\hat{\mathbf{u}}}(t) = \hat{\phi}_{\hat{\mathbf{u}}}(kt)$ for all $t \geq 0$ and $\hat{\mathbf{u}}$. Letting $\hat{\mathbf{u}}$ be the control signal such that $\hat{\phi}_{\hat{\mathbf{u}}}(kt) = z \in \partial\hat{\mathcal{R}}^T(x_0)$, the statement follows immediately. ■

Remark C.3: The uniform scaling from any ball-shaped set to a unit ball does not affect the analysis technique used to obtain the proxy system, whose reachable set is guaranteed to be a subset of the true reachable set. In view of Corollary C.2, when working with the proxy system, a uniform scaling of the input set only affects the guaranteed reachable time. ◊

APPENDIX D
REACHABILITY ANALYSIS

For a that cannot satisfy (7), differences arise in the control design at τ_n . In this case, we create a reference path for $\phi_{\mathbf{u}}(t) - at$ by using controller $\frac{y-aT}{|y-aT|}$ in the proxy system to reach $y \in \hat{\mathcal{R}}_{\text{pse}}^T(x_0)$. The reference path then becomes the line segment from x_0 to $y - aT$. We also use a piecewise constant control signal \mathbf{u} that ensures $\dot{d}_{z_n}(\phi_{\mathbf{u}}(t, \mathbf{x}_n) - at) < 0$ for all $t \in [\tau_n, \tau_{n+1})$ and for each n . In addition, we have the following inductive result as a slight modification of Lemma 4.2.

Lemma D.1: For each $n \geq 1$, let $\mathbf{x}_n := x_{n,0} - a\tau_n$ be given and consider $z_n = \theta_n(y - aT)$ with $|z_n - \mathbf{x}_n| = r$ for some $\theta_n \geq 0$. Given that $d_{z_n}(\phi_{\mathbf{u}}(t)) < a$ for all $t \in [\tau_n, \tau_{n+1})$. Then, there exists a $z_{n+1} = \theta_{n+1}(y - aT)$ such that $\theta_{n+1} > \theta_n$ and $|z_{n+1} - \mathbf{x}_{n+1}| = r$. ◊

We summarize the algorithm in Algorithm 2.

Algorithm 2 Control Synthesis

Require: $d, m, x_{0,0} := x_0, T, y \in \partial\hat{\mathcal{R}}_{\text{pse}}^T(x_0)$, and $u_{0,0} =$

$$(1 - \epsilon) \frac{G(x_0)^\dagger (y - aT - x_0)}{\|G(x_0)^\dagger\| \|y - aT - x_0\|}.$$

Require: $\delta t, \epsilon, k$ based on the conditions $\epsilon > (C_3/C)\delta t$, $\frac{2kb\tau}{b-c\rho} < T$, $k > \frac{Cb}{b-c\rho}$, and $\mathcal{E}_n(\delta t, \epsilon) + \mathcal{E}_\mu(\delta t, \epsilon) \leq r(b - c|\mathbf{x}_n| - \mathcal{E}_r(\delta t, \epsilon) + \epsilon M_0)$, where $r = \sup_{\{\hat{\mathbf{u}} \equiv \hat{\mathbf{u}} \in \partial\hat{\mathcal{U}}\}} |\phi_{\mathbf{u}}(k(m+1)\delta t, x_0) - ak(m+1)\delta t - x_0|$. $n = 0$.

2: **repeat**

$$\tau_n = n(m+1)\delta t.$$

4: **for** j **from** 0 **to** m **do**

$$\mathbf{u}([\tau_n + j\delta t, \tau_n + (j+1)\delta t]) \equiv u_{n,j} \text{ (see Eq. (4));}$$

6: $x_{n,j+1} = \phi_{\mathbf{u}}(\delta t, x_{n,j})$.

end for

8: $\mathbf{x}_{n+1} = x_{n,m+1} - a(\tau_n + (m+1)\delta t)$.

Determine z_{n+1} based on Lemma D.1.

10: Let $u_{n+1,0} = (1 - \epsilon) \arg\min_{u \in \mathcal{U}_\lambda} \langle 2(\mathbf{x}_{n+1} - z_{n+1}), \sum_{j \in \mathcal{I}} \lambda_j (x_{n,j+1} - x_{n,j}) \rangle$, where $\sum_{j \in \mathcal{I}} \lambda_j = 1$ and \mathcal{U}_λ are defined in Definition 4.1.

$$n := n + 1.$$

12: **until** $n(m+1)\delta t \geq T$.

Proposition D.2: Following Algorithm 2, $\phi_{\mathbf{u}}$ will reach $\mathcal{B}^d(y; \gamma(k, \delta t, \epsilon))$, where $\gamma(k, \delta t, \epsilon) := N\nu(\delta t) + (rcN\nu(\delta t) +$

$rC_r(\delta t, \epsilon) + C_n(\delta t, \epsilon) + \mathcal{E}_\mu(\delta t, \epsilon)\tau$, N is the number of iteration where the algorithm stops, $\nu(\delta t) = C_1\delta t - \bar{r}$, and \bar{r} is the minimum distance for (3) to travel under a constant signal $\hat{\mathbf{u}}$ with $|\hat{\mathbf{u}}| \equiv 1$ within the time horizon τ . \diamond

Proof: For each n , let $\mathbf{u}(t) = u_{n,j}$ for $t \in [\tau_n + j\delta t, \tau_n + (j+1)\delta t]$ and for $j \in \mathcal{I}$. One can show in the same way as in Corollary 4.8 that $\dot{d}_{z_n}(\phi_{\mathbf{u}}(t)) < a$ for all $t \in [\tau_n, \tau_{n+1})$ and for each n .

Now we introduce $\{\tilde{z}_n\}$ with $\tilde{z}_n = \theta_n(y - aT)$ for $\theta_n \geq 0$ for the flow $\hat{\phi}_{\hat{\mathbf{u}}}(t) - at$ as in Lemma D.1, where $\hat{\mathbf{u}} \equiv \frac{y-aT}{|y-aT|}$. Let $\hat{r}_n := |\hat{\phi}_{\hat{\mathbf{u}}}(\tau_n) - \hat{\phi}_{\hat{\mathbf{u}}}(\tau_{n-1})|$ for each n . We compare the distances related to $\hat{\phi}_{\hat{\mathbf{u}}}(t) - at$ and $\phi_{\mathbf{u}}(t) - at$.

Note that $|\hat{\phi}_{\hat{\mathbf{u}}}(t) - \phi_{\mathbf{u}}(t)| = \mathcal{O}(\delta t)$ for $t \in [0, \tau]$ and $|\tilde{z}_1 - z_1| = \mathcal{O}(\delta t)$. We can show inductively that, for $t \in [\tau_n, \tau_{n+1}]$, $|\hat{\phi}_{\hat{\mathbf{u}}}(t) - \phi_{\mathbf{u}}(t)| \leq n(C_1\delta t - \hat{r}_n) + n\mathcal{O}(\delta t) =: n\nu(\delta t)$, which implies $|\tilde{z}_n - z_n| \leq n\nu(\delta t)$.

By a direct comparison with (11), we have

$$\begin{aligned} & |\dot{d}_{\tilde{z}_n}(\hat{\phi}_{\hat{\mathbf{u}}}(t) - at) - \dot{d}_{z_n}(\phi_{\mathbf{u}}(t) - at)| \\ & \leq rc|\hat{\phi}_{\hat{\mathbf{u}}}(t) - \phi_{\mathbf{u}}(t)| + r \cdot C_r(\delta t, \epsilon) + C_n(\delta t, \epsilon) + \mathcal{E}_\mu(\delta t, \epsilon). \end{aligned} \quad (12)$$

Let $\rho(k, \delta t, \epsilon, n) := rcn\nu(\delta t)\tau + r\tau C_r(\delta t, \epsilon) + \tau C_n(\delta t, \epsilon) + \tau\mathcal{E}_\mu(\delta t, \epsilon)$. It follows that

$$\begin{aligned} & ||\hat{\phi}_{\hat{\mathbf{u}}}(t) - at - \tilde{z}_n| - |\phi_{\mathbf{u}}(t) - at - z_n|| \\ & \leq \int_0^\tau |\dot{d}_{\tilde{z}_n}(\hat{\phi}_{\hat{\mathbf{u}}}(t)) - \dot{d}_{z_n}(\phi_{\mathbf{u}}(t))| dt \leq \rho(k, \delta t, \epsilon, n). \end{aligned} \quad (13)$$

Let N be such that $\tau_N \leq T \leq \tau_{N+1}$. Then, $\phi_{\mathbf{u}}(T) = \phi_{\mathbf{u}}(T) - z_N + z_N - z_{N-1} + z_{N-1} - z_{N-1} + \dots$. Due to the monotone direction of $\{z_n\}$, we have that $\phi_{\mathbf{u}}(T) = \phi_{\mathbf{u}}(T) - z_N + \sum_{n=1}^N |z_n - z_{n-1}| \hat{\mathbf{u}} = \phi_{\mathbf{u}}(T) - z_N + \sum_{n=1}^N |\tilde{z}_n - \tilde{z}_{n-1}| \hat{\mathbf{u}} + N\nu(\delta t) \hat{\mathbf{u}} = \phi_{\mathbf{u}}(T) - z_N + \tilde{z}_N + N\nu(\delta t) \hat{\mathbf{u}} = \phi_{\mathbf{u}}(T) - z_N - (\hat{\phi}_{\hat{\mathbf{u}}}(T) - \tilde{z}_N) + y + N\nu(\delta t) \hat{\mathbf{u}}$. Therefore,

$$\begin{aligned} & |\phi_{\mathbf{u}}(T) - y| \\ & \leq ||\hat{\phi}_{\hat{\mathbf{u}}}(T) - at - \tilde{z}_N| - |\phi_{\mathbf{u}}(T) - at - z_N|| + N\nu(\delta t) \\ & \leq \gamma(k, \delta t, \epsilon) \end{aligned} \quad (14)$$

which completes the proof. \blacksquare

Remark D.3: The term γ is dominated by $N\nu(\delta t)$, where N is proportional to T . The accuracy of reachability control maintains its precision only within a sufficiently small time horizon. This limitation arises not from any deficiency in the algorithm itself, but because our aim is to leverage the knowledge of the GRS based on (3). Unfortunately, the precision suffers due to the inherent inaccuracies in GRS estimation for large values of a . \diamond